Imaging Science in Dentistry 2018; 48: 177-84
https://doi.org/10.5624/isd.2018.48.3.177

Influence of voxel size on cone-beam computed tomography-based detection of vertical root fractures in the presence of intracanal metallic posts

Fernanda Paula Yamamoto-Silva[1], Claudeir Felipe de Oliveira Siqueira[1], Maria Alves Garcia Santos Silva[1], Rodrigo Borges Fonseca[2], Ananda Amaral Santos[1], Carlos Estrela[1], Brunno Santos de Freitas Silva[3,*]

[1]*Department of Stomatologic Sciences, School of Dentistry, Federal University of Goiás, Goiânia, Brazil*
[2]*Department of Oral Rehabilitation, Dental School, Federal University of Goiás, Goiânia, Brazil*
[3]*Department of Oral Pathology, School of Dentistry, University of Anápolis, Anápolis, Brazil*

ABSTRACT

Purpose: This study was performed to evaluate the influence of voxel size and the accuracy of 2 cone-beam computed tomography (CBCT) systems in the detection of vertical root fracture (VRF) in the presence of intracanal metallic posts.

Materials and Methods: Thirty uniradicular extracted human teeth were selected and randomly divided into 2 groups (VRF group, n = 15; and control group, n = 15). The VRFs were induced by an Instron machine, and metallic posts were placed in both groups. The scans were acquired by CBCT with 4 different voxel sizes: 0.1 mm and 0.16 mm (for the Eagle 3D V-Beam system) and 0.125 mm and 0.2 mm (for the i-CAT system) (protocols 1, 2, 3, and 4, respectively). Interobserver and intraobserver agreement was assessed using the Cohen kappa test. Sensitivity and specificity were evaluated and receiver operating characteristic analysis was performed.

Results: The intraobserver coefficients indicated good (0.71) to very good (0.83) agreement, and the interobserver coefficients indicated moderate (0.57) to very good (0.80) agreement. In respect to the relationship between sensitivity and specificity, a statistically significant difference was found between protocols 1 (positive predictive value: 0.710, negative predictive value: 0.724) and 3 (positive predictive value: 0.727, negative predictive value: 0.632) ($P < .05$). The least interference due to artifact formation was observed using protocol 2.

Conclusion: Protocols with a smaller voxel size and field of view seemed to favor the detection of VRF in teeth with intracanal metallic posts. ***(Imaging Sci Dent 2018; 48: 177-84)***

KEY WORDS: Tooth Fractures; Cone-Beam Computed tomography

Introduction

Vertical root fracture (VRF) is one of the causes of tooth loss.[1-3] Diagnosing VRF can be complex, in part because it presents with variable and nonspecific clinical and radiographic signs and symptoms. Misdiagnosing VRF could potentially result in unnecessary tooth extraction.[4]

In periapical radiographs, VRF can be observed as a vertically-oriented radiolucent line in the root that is only visible when the central X-ray beam is parallel to the fracture line.[2,5] In 2-dimensional radiographic exams, one of the main limitations in VRF detection is the superimposition of adjacent tissues and the presence of radiopaque materials in the root canal.[6] Nevertheless, these limitations can be partially supplanted by 3-dimensional views obtained using cone-beam computed tomography (CBCT).

CBCT has broadly demonstrated superior effectiveness in the diagnosis of VRF compared to periapical radiography;[7-9] however, the accuracy depends on the CBCT system used, the voxel size, the field of view (FOV), and

*This study was supported by grants from the National Council for Scientific and Technological Development (CNPq, grant 457536/2014 to F.P.Y.S.).
Received May 25, 2018; Revised July 17, 2018; Accepted July 31, 2018
*Correspondence to : Prof. Brunno Santos de Freitas Silva
Department of Oral Pathology, Dental School, University of Anápolis. Av. Universitária, km 3,5. Cidade Universitária, Anápolis, GO 75083-515, Brazil
Tel) 55-62-3310-6630, Fax) 55-62-3434-4394, E-mail) brunno.santosfreitas@gmail.com

Imaging Science in Dentistry · pISSN 2233-7822 eISSN 2233-7830

the type of radiopaque material present in the area of interest.[7,10,11] Indeed, metallic intracanal posts produce beam-hardening artifacts, which pose a real problem in the interpretation of VRF in CBCT through the induction of inaccurate images.[12]

The influence of voxel size has recently been investigated, with the goal of evaluating the accuracy of various CBCT protocols on the detection of VRF in the presence of intracanal metallic posts.[7] Although some evidence has suggested that voxel size could be significantly relevant for the diagnosis of VRF,[13] other studies have also demonstrated that smaller voxel sizes could cause some difficulties in detecting horizontal root fractures on CBCT when metallic posts are present.[14,15] These discrepancies indicate that there is still a need to examine the influence of voxel size on VRF detection, especially in the presence of metallic posts. As a consequence of the diversity of CBCT systems available on the market and the wide variation in their image quality and performance, studying the accuracy of various CBCT systems in VRF detection is considered to be of the utmost importance.[10]

Considering the scarcity of investigations into the influence of different voxel sizes on the detection of VRF in teeth with metallic posts and the lack of information about the accuracy of the Eagle 3D V-Beam (Dabi Atlante, Ribeirão Preto, São Paulo, Brazil) CBCT system in detecting VRF, this study analyzed the influence of voxel size and the accuracy of 2 CBCT systems (Eagle 3D V-Beam and i-CAT Cone Beam 3D Imaging System; Imaging Sciences International, Hatfield, PA) in the detection of VRF in the presence of intracanal metallic posts.

Materials and Methods

Sample selection

This experimental study was approved by the Human Ethics Committee of the Institutional Review Board (approval number 477.315/2017). Thirty uniradicular extracted human teeth were selected after a transillumination exam, an inspection of the external surface of roots with a surgical microscope (OPMI, Zeiss, Oberkochen, Germany), and a digital radiographic exam (Focus, Kavo, Instrumentarium Dental, Tuusula, Finland). Teeth with signs of cracks, root fracture, root resorption, supernumerary roots, internal calcification, canal obliteration, or incomplete root formation were excluded from the sample. The selected teeth were immersed for 30 minutes in 5% sodium hypochlorite (Fitofarma, Goiânia, GO, Brazil), solution, and then underwent scaling and root planing to eliminate remaining organic tissue and dental calculus.

Sample preparation

The crowns of all teeth were removed at the cementoenamel junction and the root canals were prepared with the ProTaper rotary system (Dentsply Maillefer, Tulsa, OK, USA) under copious irrigation with distilled water up to size F3. The root canals were filled with gutta-percha cones (Dentsply Maillefer, Ballaigues, Switzerland) by cold lateral compaction with epoxy-amine resin sealer (AH Plus; Dentsply, Konstanz, Germany). Seven days after obturation, two-thirds of the root length was prepared with the intent to create the post space. The posts and cores were fabricated with Duralay (Reliance Dental Manufacturing, Worth, IL, USA), and subsequently placed into a cast of nickel-chromium alloy. The metallic posts were then gently cemented in each tooth. At this time, the samples were randomly divided into 2 groups of 15 teeth each (the VRF group and the control group).

In the VRF group, the periodontal ligament was simulated before induction of the fracture, as described previously.[16] The VRF was then induced by an Instron machine (Instron, TTDML®, Canton, MA, USA) by using a 2000 kilogram-force load cell and a cross-speed of 0.5 mm/min. After confirmation of the fracture, fragments that showed complete separation were glued with cyanoacrylate cement (Loctite®, Henkel Ltda., Sao Paulo, SP, Brazil).

CBCT image acquisition

Each tooth (VRF group, n = 15; and control group, n = 15) was individually placed in the same empty socket of an edentulous dry human mandible. The mandible with the placed tooth was immersed in a plastic cylinder container filled with water to simulate soft tissue attenuation, as described previously.[5]

The scans were acquired by the Eagle 3D V-Beam system and the i-CAT Cone Beam 3D Imaging System (Fig. 1). Each sample was scanned using the following exposure protocol: Eagle 3D – 5- × 5-cm FOV, 32 seconds, 85 kVp, 5 mA, and 2 different voxel sizes, 0.1 mm (protocol 1) and 0.16 mm (protocol 2); i-CAT – 8- × 8-cm FOV, 26.9 seconds, 120 kVp, 5 mA, and 2 different voxel sizes, 0.125 mm (protocol 3) and 0.2 mm (protocol 4). Two calibrated oral radiologists, blinded to the protocol, with 5 and 30 years of experience, randomly evaluated the entire volume in the axial, coronal, and sagittal planes. The images were analyzed individually in a quiet and darkened room using InVivo Dental Application software (version

Fig. 1. Images of vertical root fracture with a metallic post in 2 cone-beam computed tomography systems with different voxel sizes. Protocol 1 with 0.1-mm voxels in (A) the axial plane (A), the coronal plane (B), and the cross-sectional plane (C). Protocol 2 with 0.16-mm voxels in the axial plane (D), the coronal plane (E), and the cross-sectional plane (F). Protocol 3 with 0.125-mm voxels in the axial plane (G), the coronal plane (H), and the cross-sectional plane (I). Protocol 4 with 0.2-mm voxels in the axial plane (J), the coronal plane (K), and the cross-sectional plane (L).

5.3.2, Anatomage Inc., San Jose, CA, USA) on a Dell XPS X8700 computer, with a 3.4 GHz Intel Core i7-4770 Processor, 12GB DDR3 memory, 2TB HDD, an NVIDIA GeForce GTX 645 graphics card (Dell Inc., Austin, TX, USA), and a 28-inch color monitor (UltraHD, Dell Inc., Austin, TX, USA).

The presence of VRF was scored on a 5-point scale: 1, VRF definitely absent; 2, VRF probably absent; 3, uncertain; 4, VRF probably present; 5, VRF definitely present. The level of interference due to image artifacts with VRF detection was then analyzed and scored on a 3-point scale: 1, no interference; 2, slight interference; and 3, severe interference. Additionally, the oral radiologists indicated which orientation contributed more to VRF detection: axial, coronal, or sagittal. A second evaluation was performed in 50% of the samples.

Statistical analysis

The data were analyzed using SPSS® version 21 (IBM Corp., Armonk, NY, USA). Interobserver and intraobserver agreement was assessed using the Cohen kappa test, and the values were interpreted as follows: 0 to 0.20, weak agreement; 0.21 to 0.40, fair agreement; 0.41 to 0.60,

Table 1. Kappa test values for the agreement between scanning protocols and cone-beam computed tomography (CBCT) systems in vertical root fracture detection

CBCT system	Voxel size, mm	FOV, cm	Kappa value	*P*
Eagle 3D	0.1	5×5	0.8	<0.05
Eagle 3D	0.16	5×5	0.76	
i-CAT	0.125	8×8	0.57	
i-CAT	0.2	8×8	0.63	

FOV: field of view

Table 2. Area under the receiver operating characteristic curve (AUC) for the different cone-beam computed tomography protocols in vertical root fracture detection and the respective confidence intervals

Protocol	AUC	*P*	95% CI
Eagle 3D, voxel: 0.1 mm	0.784	0.001	0.651-0.917
Eagle 3D, voxel: 0.16 mm	0.513	0.876	0.350-0.676
i-CAT, voxel: 0.125 mm	0.729	0.006	0.582-0.875
i-CAT, voxel: 0.2 mm	0.458	0.611	0.296-0.619

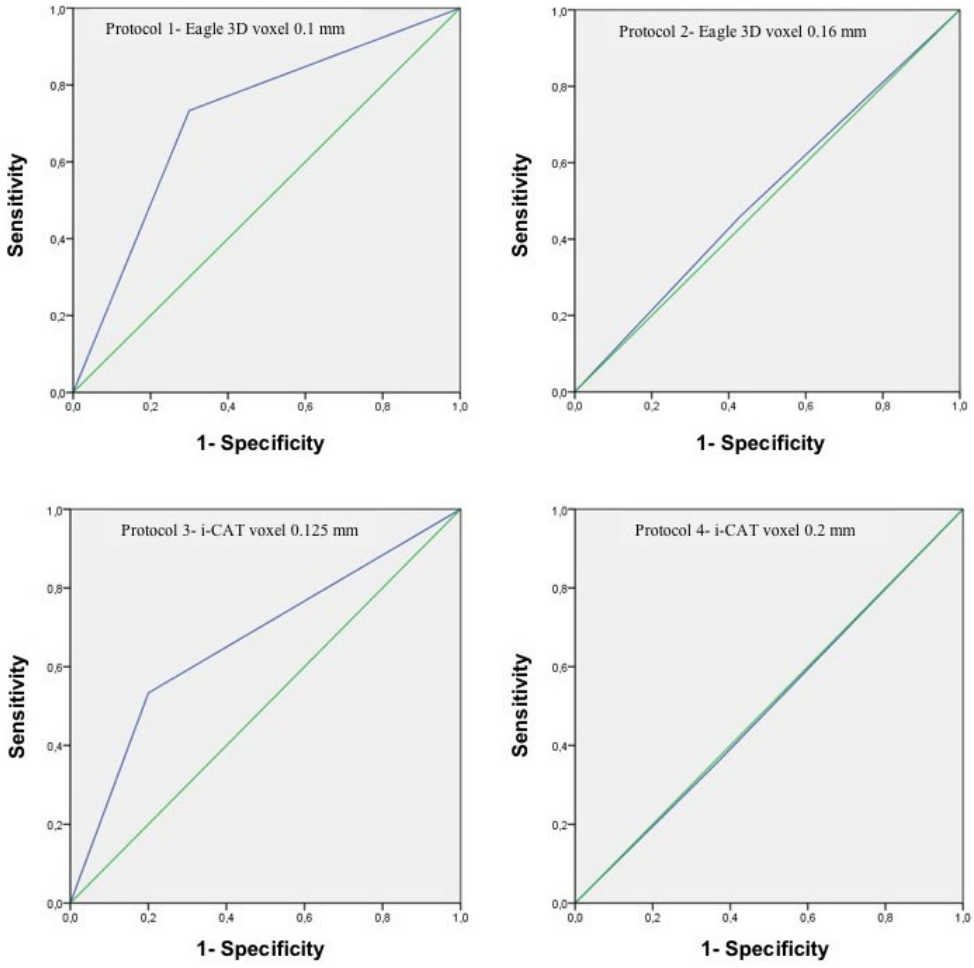

Fig. 2. Receiver operating characteristic curves of the scanning protocols and cone-beam computed tomography systems.

Table 3. Sensitivity, specificity, positive predictive value (PPV), negative predictive value (NPV), and accuracy for each scanning protocol

Protocol	Sensitivity	Specificity	PPV	NPV	Accuracy
Eagle 3D, voxel: 0.1 mm	0.733	0.700	0.710	0.724	0.717
Eagle 3D, voxel: 0.16 mm	0.458	0.571	0.478	0.552	0.519
i-CAT, voxel: 0.125 mm	0.530	0.800	0.727	0.632	0.666
i-CAT, voxel: 0.2 mm	0.357	0.633	0.476	0.514	0.500

Table 4. Interference of artifact formation in the diagnosis of vertical root fracture between the cone-beam computed tomography protocols

Protocols	Frequency of artifact interference levels (%)			P^*	P^{**}
	No interference	Slight interference	Severe interference		
Eagle 3D, voxel: 0.1 mm	23.3%	23.3%	53.3%	0.005	0.355
Eagle 3D, voxel: 0.16 mm	35.2%	42.6%	22.2%	0.179	0.560
i-CAT, voxel: 0.125 mm	25.0%	31.7%	43.3%	0.212	0.658
i-CAT, voxel: 0.2 mm	20.7%	20.7%	58.6%	0.001	0.843

*: Chi-square; **: Analysis of variance

moderate agreement; 0.61 to 0.80, good agreement; 0.81 to 0.99, very good agreement; and 1, perfect agreement. To assess intraobserver agreement, the same evaluation was repeated under identical conditions after 2 weeks.

Sensitivity and specificity were evaluated, and receiver operating characteristic (ROC) analysis was performed. The results were compared using 2-way analysis of variance (ANOVA) and the *post hoc* Tukey test. For the analysis of interference from image artifacts in VRF detection, and which orientation contributed most to VRF detection, 1-way ANOVA was applied. For all analyses, P values $< .05$ were considered to indicate statistical significance.

Results

The intraobserver coefficient indicated good (0.71) to very good (0.83) agreement, and the inter-observer coefficient indicated good (0.74) to very good (0.80) agreement for VRF diagnosis ($P < 0.05$). Regarding the agreement observed between each scanning protocol and the CBCT system, the coefficient indicated moderate to very good agreement (Table 1).

To evaluate the relationship between sensitivity and specificity, the area under the ROC curve was calculated for the various scanning protocols. A statistically significant difference was found between protocols 1 and 3 ($P < .05$), which also presented the highest values of the area under the ROC curve (Table 2, Fig. 2).

The sensitivity, specificity, positive predictive value, negative predictive value, and accuracy of each scanning protocol are presented in Table 3.

In the radiologists' evaluation of interference due to artifact formation in the diagnosis of VRF, it was observed that protocol 2 showed the least interference. In protocols 1 and 4, interference was more frequent ($P < .05$) (Table 4). No statistically significant trends were found regarding the most efficient orientation (axial, coronal, or sagittal) for VRF detection.

Discussion

Diagnosing VRF is a challenging task due to its nonspecific signs and symptoms, especially in cases without evident separation of the adjacent segments, as well as due to limitations in its detection using 2-dimensional radiographic exams.[8,9,17,18] Although CBCT has demonstrated greater effectiveness in VRF detection, in cases where metallic intracanal posts are present, the interpretation of these fractures can be problematic because of the presence of image artifacts.[5,19] Voxel size is one of the many factors that can influence root fracture detection in the presence of metallic posts.[14,15]

The results of this study suggest that protocols with a smaller voxel size are more accurate for VRF detection in the presence of metallic intracanal posts. Indeed, the small voxel size protocols presented in this study showed significantly higher specificity. This means that using these smaller-voxel protocols to detect VRF could confirm true positive cases. Voxel size can directly influence

the visualization of root fractures, presenting a positive correlation with image quality and influencing spatial and contrast resolution.[20,21] Theoretically, small voxel reconstructions could be associated with a high level of image artifacts in the presence of a metallic material. This could be explained by the tendency for the limited number of photons within a small voxel to increase the extent of image artifacts.[15,22] The greater accuracy in VRF detection in the presence of metallic posts found in the present study could be explained by other parameters than just the voxel size. Several parameters can influence the quality of CBCT images and VRF detection, such the size of the FOV, the type of detector, and the CBCT system.[20,22]

In the last 5 years, several studies have aimed to evaluate the influence of certain CBCT parameters on the detection of VRF in the presence of metallic intracanal posts.[2,5,7,20,11,19,23-25] According to Junqueira et al. (2013),[7] voxel size did not influence the detection of VRF in the presence of a metallic post. However, in their study, greater sensitivity was associated with a small-voxel protocol (i-Cat Next Generation – 5-×5-cm FOV, 120 kVp, with a 0.125-mm voxel size). Neves et al. (2014)[5] evaluated 4 different imaging modes of the 3D Accuitomo 170 CBCT system (4-×4-cm FOV, 90 kVp, with a 0.08-mm voxel size) in VRF detection. They did not found any improvement in the ability of CBCT to detect VRF in teeth with metallic materials when any of the imaging modes were applied. In fact, it is important to keep in mind that some metal reduction algorithms available in CBCT systems could exert a negative influence on the accuracy of root fracture detection,[26] or may not have any influence on VRF detection in the presence of metallic artifacts.[11]

In the investigation of Jakobson et al. (2014),[10] the accuracy of 2 CBCT systems (NewTom 3G – 15-×24-cm FOV, 110 kVp, 0.2-mm voxel size; and i-Cat Next Generation – 8-cm FOV, 120 kVp, and 0.2-mm voxel size) in the detection of VRF with the presence of metallic posts was analyzed. They suggested that systems with a small FOV could enhance the detection of VRF in the presence of metallic posts. This is a plausible proposal, since small FOV protocols have higher resolution and contrast than large FOV devices.[27] The authors assumed that the detector design technology of the NewTom 3G, with a tube/charge-coupled device, could be inferior to the flat-panel detector of the i-Cat Next Generation system.[10] According to them, the NewTom 3G panel detector had a lower dynamic range, contrast, and spatial resolution and higher levels of pixel noise and image artifacts, which could negatively affect VRF detection.[10]

Safi et al. (2015)[23] also analyzed the accuracy of 2 CBCT systems in the detection of VRF in the presence of metallic artifacts: NewTom VGI (12-×8-cm FOV, 90 kVp, 0.2-mm voxel size) and Scanora 3D CBCT systems (10-×7.5-cm FOV, 110 kVp, and 0.2-mm voxel size). In their study, the interobserver agreement was almost perfect, with no significant differences in the accuracy of the 2 CBCT systems in the detection of VRF associated with metal posts. However, the extensive experience of the observers in their study might have positively influenced the detection of VRF, which could explain the similar accuracy of the 2 CBCT systems.

The influence of CBCT enhancement filters (i-Cat Next Generation – 8-×8-cm FOV, 120 kVp, and 0.2-mm voxel size) on the diagnosis of VRF in teeth with intracanal metallic posts was studied by Ferreira et al. (2015).[2] These filters did not significantly improve the diagnosis of VRF in the presence of metallic posts. Despite their conclusions, enhancement filters are widely employed in CBCT images, with beneficial results in the diagnosis of VRF in teeth without metallic artifacts.[28]

The exposure parameters used in CBCT scans and their relationship with VRF detection in the presence of metallic posts have recently been addressed.[19] Although adjusting certain exposure parameters could contribute to avoiding lower-energy photons and reducing artifact formation, variation in these parameters did not influence VRF detection in the presence of root canal metallic materials.[19] In contrast, Safi et al. (2016)[25] found that lower-amperage (4 mA) protocols combined with a smaller FOV (7.5 cm) were more accurate for VRF detection in teeth with metallic posts. In this study, only 2 CBCT systems were tested with a static 5 mA parameter, to remove variation due to this parameter from the analysis of VRF detection.

A range of CBCT systems are available on the market, with wide variation in their performance in terms of image quality. The present study presented some novel information about the accuracy of the Eagle 3D V-Beam system in detecting VRF in teeth with metallic posts. The Eagle 3D V-Beam system more accurately detected VRF in the presence of metallic posts than the i-CAT Cone Beam 3D Imaging System. This could be explained by the possibility that the scanning parameters available in the Eagle 3D V-Beam system may have been favorable for VRF detection performance. This premise is based on the fact that with the Eagle-3D it was possible to work with 0.1-mm voxels and an FOV of 5×5 cm, unlike the present i-CAT system, for which we used 0.125-mm vox-

els and an FOV of 8 × 8 cm. Regarding the detector technology, the 2 CBCT systems analyzed in this study contained a flat-panel sensor, with the Eagle 3D system using a complementary metal-oxide semiconductor device and the i-Cat system using an amorphous silicon flat-panel sensor with a CsI scintillator. In general, flat-panel sensors offer less peripheral distortion and less image noise.[29]

As only 2 CBCT systems were included in the present investigation, we did not intend to fully explore all the technical parameters that may influence the accuracy of CBCT in VRF detection. Although several factors can influence the quality of CBCT images, voxel size seems important to investigate for the detection of VRF in the presence of metallic artifacts. Although we found that protocols with smaller voxels were more accurate for VRF detection, it is important to emphasize that we also found some divergences regarding which protocol presented less interference due to artifact formation.

In summary, it seems that protocols and CBCT systems with a smaller voxel size and FOV favor the detection of VRF in teeth with intracanal metallic posts.

References

1. Chai H, Tamse A. The effect of isthmus on vertical root fracture in endodontically treated teeth. J Endod 2015; 41: 1515-9.
2. Ferreira LM, Visconti MA, Nascimento HA, Dallemolle RR, Ambrosano GM, Freitas DQ. Influence of CBCT enhancement filters on diagnosis of vertical root fractures: a simulation study in endodontically treated teeth with and without intracanal posts. Dentomaxillofac Radiol 2015; 44: 20140352.
3. Fuss Z, Lustig J, Katz A, Tamse A. An evaluation of endodontically treated vertical root fractured teeth: impact of operative procedures. J Endod 2001; 27: 46-8.
4. Chang E, Lam E, Shah P, Azarpazhooh A. Cone-beam computed tomography for detecting vertical root fractures in endodontically treated teeth: a systematic review. J Endod 2016; 42: 177-85.
5. Neves FS, Freitas DQ, Campos PS, Ekestubbe A, Lofthag-Hansen S. Evaluation of cone-beam computed tomography in the diagnosis of vertical root fractures: the influence of imaging modes and root canal materials. J Endod 2014; 40: 1530-36.
6. Metska ME, Aartman IH, Wesselink PR, Özok AR. Detection of vertical root fractures in vivo in endodontically treated teeth by cone-beam computed tomography scans. J Endod 2012; 38: 1344-7.
7. Junqueira RB, Verner FS, Campos CN, Devito KL, do Carmo AM. Detection of vertical root fractures in the presence of intracanal metallic post: a comparison between periapical radiography and cone-beam computed tomography. J Endod 2013; 39: 1620-4.
8. D'Addazio PS, Campos CN, Özcan M, Teixeira HG, Passoni RM, Carvalho AC. A comparative study between cone-beam computed tomography and periapical radiographs in the diagnosis of simulated endodontic complications. Int Endod J 2011; 44: 218-24.
9. Wang P, Yan XB, Lui DG, Zhang WL, Zhang Y, Ma XC. Detection of dental root fractures by using cone-beam computed tomography. Dentomaxillofac Radiol 2011; 40: 290-8.
10. Jakobson SJ, Westphalen VP, Silva-Neto UX, Fariniuk LF, Schroeder AG, Carneiro E. The influence of metallic posts in the detection of vertical root fractures using different imaging examinations. Dentomaxillofac Radiol 2014; 43: 20130287.
11. de Rezende Barbosa GL, Sousa Melo SL, Alencar PN, Nascimento MC, Almeida SM. Performance of an artefact reduction algorithm in the diagnosis of in vitro vertical root fracture in four different root filling conditions on CBCT images. Int Endod J 2016; 49: 500-8.
12. Bueno MR, Estrela C, De Figueiredo JA, Azevedo BC. Map-reading strategy to diagnose root perforations near metallic intracanal posts by using cone beam computed tomography. J Endod 2011; 37: 85-90.
13. Kamburoğlu K, Murat S, Yüksel SP, Cebeci AR, Horasan S. Detection of vertical root fracture using cone-beam computerized tomography: an in vitro assessment. Oral Surg Oral Med Oral Pathol Oral Radiol Endod 2010; 109: e74-81.
14. Costa FF, Gaia BF, Umetsubo OS, Pinheiro LR, Tortamano IP, Cavalcanti MG. Use of large-volume cone-beam computed tomography in identification and localization of horizontal root fracture in the presence and absence of intracanal metallic post. J Endod 2012; 38: 856-9.
15. Costa FF, Gaia BF, Umetsubo OS, Cavalcanti MG. Detection of horizontal root fracture with small-volume cone-beam computed tomography in the presence and absence of intracanal metallic post. J Endod 2011; 37: 1456-9.
16. Naves LZ, Silva GR, Correr-Sobrinho L, Costa AR, Valdivia AD, Soares CJ. Influence of crosshead speed on failure load and failure mode of restored maxillary premolars. Braz Oral Res 2016; 30. pii: S1806-83242016000100206.
17. Khedmat S, Rouhi N, Drage N, Shokouhinejad N, Nekoofar MH. Evaluation of three imaging techniques for the detection of vertical root fractures in the absence and presence of gutta-percha root fillings. Int Endod J 2012; 45: 1004-9.
18. Chavda R, Mannocci F, Andiappan M, Patel S. Comparing the in vivo diagnostic accuracy of digital periapical radiography with cone-beam computed tomography for the detection of vertical root fracture. J Endod 2014; 40: 1524-9.
19. Pinto MG, Rabelo KA, Sousa Melo SL, Campos PS, Oliveira LS, Bento PM, et al. Influence of exposure parameters on the detection of simulated root fractures in the presence of various intracanal materials. Int Endod J 2017; 50: 586-94.
20. Elsaltani MH, Farid MM, Eldin Ashmawy MS. Detection of simulated vertical root fractures: which cone-beam computed tomographic system is the most accurate? J Endod 2016; 42: 972-7.
21. Katsumata A, Hirukawa A, Okumura S, Naitoh M, Fujishita M, Ariji E, et al. Relationship between density variability and imaging volume size in cone-beam computerized tomographic scanning of the maxillofacial region: an in vitro study. Oral Surg Oral Med Oral Pathol Oral Radiol Endod 2009; 107:

420-5.
22. Tanimoto H, Arai Y. The effect of voxel size on image reconstruction in cone-beam computed tomography. Oral Radiol 2009; 25: 149-53.
23. Safi Y, Aghdasi MM, Ezoddini-Ardakani F, Beiraghi S, Vasegh Z. Effect of metal artifacts on detection of vertical root fractures using two cone beam computed tomography systems. Iran Endod J 2015; 10: 193-8.
24. Menezes RF, Araújo NC, Santa Rosa JM, Carneiro VS, Santos Neto AP, Costa V, et al. Detection of vertical root fractures in endodontically treated teeth in the absence and in the presence of metal post by cone-beam computed tomography. BMC Oral Health 2016; 16: 48.
25. Safi Y, Hosseinpour S, Aziz A, Bamedi M, Malekashtari M, Vasegh Z. Effect of amperage and field of view on detection of vertical root fracture in teeth with intracanal posts. Iran Endod J 2016; 11: 202-7.
26. Bechara B, Alex McMahan C, Moore WS, Noujeim M, Teixeira FB, Geha H. Cone beam CT scans with and without artefact reduction in root fracture detection of endodontically treated teeth. Dentomaxillofac Radiol 2013; 42: 20120245.
27. Hassan B, Metska ME, Ozok AR, van der Stelt P, Wesselink PR. Comparison of five cone beam computed tomography systems for the detection of vertical root fractures. J Endod 2010; 36: 126-9.
28. Nascimento MC, Nejaim Y, de Almeida SM, Bóscolo FN, Haiter-Neto F, Sobrinho LC, et al. Influence of cone beam CT enhancement filters on diagnosis ability of longitudinal root fractures. Dentomaxillofac Radiol 2014; 43: 20130374.
29. Scarfe WC, Farman AG. What is cone-beam CT and how does it work? Dent Clin North Am 2008; 52: 707-30.